Polycomb group proteins confer robustness to aposematic coloration in the milkweed bug, *Oncopeltus fasciatus*

Marie Tan, Laura Park, Elizabeth Chou, Madeline Hoesel, Lyanna Toh, Yuichiro Suzuki*

Department of Biological Sciences, Wellesley College, 106 Central St., Wellesley MA 02481, USA

* Corresponding author: email: ysuzuki@wellesley.edu; Tel: (781)283-3100

ABSTRACT

Aposematic coloration offers an opportunity to explore the molecular mechanisms underlying canalization. In this study, the role of epigenetic regulation underlying robustness was explored in the aposematic coloration of the milkweed bug, *Oncopeltus fasciatus. Polycomb* (*Pc*) and *Enhancer of Zeste* (*E(z)*), which encode components of the Polycomb Repressive Complex 1 (PRC1) and PRC2, respectively, and *jing*, a component of the PRC2.2 subcomplex, were knocked down in the fourth instar of *O. fasciatus*. Knockdown of these genes led to alterations in scutellar morphology and melanization. In particular, when *Pc* was knocked down, the adults developed a highly melanized abdomen, head, and forewings at all temperatures examined. In contrast, the *E(z)* and *jing* knockdown led to increased plasticity of the dorsal forewing melanization across different temperatures. Moreover, *jing* knockdown adults exhibited increased plasticity in the dorsal melanization of the head and the thorax. These observations demonstrate that histone modifiers may play a key role during the process of canalization to confer robustness in the aposematic coloration.

KEYWORDS: Aposematic coloration, robustness, phenotypic plasticity, Polycomb group proteins, canalization, *Oncopeltus fasciatus*

BACKGROUND

Many organisms have warning coloration to advertise their unpalatability and/or toxicity (Stevens and Ruxton, 2012). These warning colors, called aposematic coloration, are characterized by conspicuous coloration and contrasts in colors, which are more easily recognized and remembered by predators (Stevens & Ruxton, 2012). The evolution of aposematic coloration has long been debated because individuals with novel aposematic coloration among a cryptic population would be at higher risk of potential predation before predators developed an association between coloration and distastefulness (Guilford, 1988; Harvey et al., 1982; Sillen-Tullberg and Bryant, 1983). Intermediate steps involving facultative displays of aposematism have been proposed to overcome this issue. In some vertebrates, hidden aposematic coloration, where aposematic coloration is confined to specific locations on an otherwise cryptic body, have been suggested to serve as intermediate steps in the evolution of aposematism (Loeffler-Henry et al., 2023). In other cases, phenotypically plastic aposematism (Fabricant et al., 2018; Lindstedt et al., 2010, 2009; Sword, 2002) may allow aposematism to be expressed in a condition-dependent manner, such as only when the density of the prey is high (Sword, 2002). In the latter cases, selection should favor the eventual evolution of robust coloration from previously plastic traits to facilitate learning and recognition by potential predators (Sword, 2002). Many species in fact exhibit robust genetically determined aposematic coloration (Mallet, 1989; Nokelainen et al., 2013).

The evolution of robust phenotypes from environmentally induced, phenotypically plastic traits is a process known as genetic assimilation (Waddington, 1942; 1956; 1953). Phenotypically plastic traits readily change their phenotypes in response to the environment. Over time, if a specific trait confers higher fitness, then the trait will become genetically

stabilized by a process known as canalization so that the trait becomes robust to environmental and genetic perturbations (Waddington, 1942). Given the selective advantage of being robust, aposematic coloration in many species is likely to be canalized, and therefore offers an opportunity to study the molecular underpinnings of canalization.

Recent studies have suggested that chromatin structure can influence phenotypic plasticity and robustness of traits (Vogt, 2022). Chromatin is the molecular structure consisting of DNA wrapped around histone octamers. Histones can be altered by chemical modifications, such as the addition or removal of acetyl, methyl and/or ubiquitin groups to histone tails. Such chemical changes cause the chromatin structure to switch between the transcriptionally active euchromatin and the transcriptionally silent heterochromatin. Histone modifiers catalyze these changes and have been implicated in the environmental sensitivity of gene expression (Turner, 2009). Polycomb group (PcG) proteins are epigenetic regulators that repress gene expression through histone methylation and ubiquitination. Their temperature responsiveness is demonstrated in *Drosophila melanogaster*, where PcG-regulated genes have typically been shown to be more actively transcribed at lower temperatures than those at higher temperatures (Bantignies et al., 2003; Chan et al., 1994; Fauvarque and Dura, 1993; although see also Voigt and Froschauer (2023) for exceptions). Because PcGs and other chromatin regulators can impact temperature-dependent gene expression changes, loci encoding these regulators as well as their targets have been shown to be under strong selective pressures and undergo adaptive evolution (Gibert et al., 2011; Harr et al., 2002; Levine and Begun, 2008; Voigt et al., 2015). PcGs have also been implicated in conferring phenotypic plasticity (Ciabrelli et al., 2017) or phenotypic robustness (Gibert et al., 2011) of various traits including melanization. Thus, PcG genes are candidates for canalization of aposematic coloration.

In insects, PcGs act through three primary protein complexes: the Polycomb Repressive Complex 1 (PRC1), PRC2 and the pleiohomeotic-repressive complex (PhoRC). The canonical PRC1 includes dRING, Polyhomeotic (Ph), Posterior sex combs (Psc) and Polycomb (Pc) (Francis et al., 2001; Shao et al., 1999). PRC1 is associated with monoubiquitination of histone H2A at lysine 119 (Wang et al., 2004). PRC2 includes Enhancer of Zeste (E(z)), Embryonic ectoderm development (EED), Suppressor of zeste (SUZ12), and Chromatin assembly factor 1, p55 subunit (Caf1-55) (Muller et al., 2002). PRC2 can associate with two additional proteins, Jing and Jarid2, which modify the activity of PRC2 (Kassis et al., 2017). PRC2 is involved in mono-, di- and trimethylation of lysine 27 on histone H3 (Muller et al., 2002).

The milkweed bug, *Oncopeltus fasciatus,* is notable for its aposematic orange and black coloration that protects against predation (Berenbaum and Miliczky, 1984; Prudic et al., 2007). Praying mantids, for example, co-occur with *O. fasciatus* and can recognize the luminance contrasts of adult *O. fasciatus* and avoid them (Berenbaum and Miliczky, 1984; Prudic et al., 2007). Adult *O. fasciatus* have black heads with a V-shaped orange pattern, black pronotum with an orange border, a black scutellum, forewings that comprise an orange proximal leathery section with a black band, and a black distal membranous portion. The black patterns are due to the deposition of melanin (Liu et al., 2016, 2014) and are unique to the adult stage. Depending on the section of the body, the melanic coloration of *O. fasciatus* exhibits variation in plasticity. The dorsal adult wing melanization is robust and is only minimally affected by rearing temperature (Sharma et al., 2016), possibly to ensure better recognition by potential predators. In contrast, the ventral adult abdominal melanization of *O. fasciatus* exhibits extensive phenotypic plasticity in response to rearing temperatures (Novak, 1955; Sharma et al., 2016). This variability

96 in plasticity of melanic patterns offers us an opportunity to probe potential mechanisms
97 underlying canalization.

98 In this study, the role of histone modification on robustness and phenotypic plasticity was
99 examined in *O. fasciatus*. As PcGs have been implicated in the temperature-dependent plasticity
100 of abdominal melanization in *D. melanogaster* (Gibert et al., 2011, 2007), we hypothesized that
101 PcGs may also play a role in plasticity and robustness of aposematic coloration of *O. fasciatus* at
102 different rearing temperatures. Prior studies in hemimetabolous insects - insects which undergo
103 incomplete metamorphosis, such as *O. fasciatus* - have found that PcGs regulate patterning and
104 specification of segmental identity during the embryonic stage (Matsuoka et al., 2015); whether
105 or not PcGs might play a role in hemimetabolous adult pigmentation has yet to be explored.
106 Therefore, we examined the role of several genes encoding members of PcGs: *Pc* and *E(z)*,
107 which encode components of PRC1 and PRC2, respectively, and *jing*, which encodes a zinc-
108 finger protein associated with the PRC2 subcomplex PRC2.2 (Kassis et al., 2017; Sedaghat et al.,
109 2002). E(z) is a histone methyltransferase, which silences gene expression through methylation
110 of histone H3 on lysine 27 (H3K27) (Cao et al., 2002; Czermin et al., 2002; Muller et al., 2002).
111 In *D. melanogaster*, E(z) has been shown to modulate temperature-sensitive target genes (Chan
112 et al., 1994). *jing*, a homolog of the mammalian *AEBP2* gene, appears to aid in optimal PRC2
113 function by stabilizing the PRC2 complex (Fischer et al., 2022). Jing has been shown to play
114 several roles during development including the development of the CNS midline, trachea,
115 proximodistal axis establishment and segmental development of legs, and wing venation in *D.*
116 *melanogaster* (Culi et al., 2006; Sedaghat et al., 2002). Importantly, Jing has also been shown to
117 modulate abdominal pigmentation in *D. melanogaster* (Culi et al., 2006).

Using RNA interference, we knocked down the expression of *Pc*, *E(z)*, and *jing*, and examined the impact on the robustness of aposematic coloration in *O. fasciatus*. These genes encode proteins in different Polycomb Repressive Complexes, and our findings indicate that they impact plasticity in distinct ways. We found that *E(z)* and *jing* knockdown led to increased plasticity and a loss of dorsal melanization robustness across a temperature gradient. In contrast, *Pc* knockdown caused increased melanization across all temperatures.

METHODS

Animals

O. fasciatus were raised at 26.5°C on organic sunflower seeds and water in plastic containers. For the temperature experiments, *O. fasciatus* were raised separately at 20°C, 26.5°C, and 33°C under a 16 h light:8 h dark photoperiod.

mRNA isolation and cDNA synthesis

Whole bodies of *O. fasciatus* were placed in TRIzol and frozen until they were processed. The RNA was isolated using standard chloroform extraction. RNA was treated with DNase (Promega), and cDNA was generated from 1 μg of the RNA using the RevertAid First Strand cDNA Synthesis Kit (Thermo Fisher) following the manufacturer's instructions.

Double stranded RNA synthesis and injection

Fragments of *Pc*, *E(z)* and *jing* were amplified using the primers listed in Table S1. The PCR products were then inserted into a TOPO TA vector (Thermo Fisher). Following the transformation of *E. coli* cells with this plasmid, the cells were grown, and the plasmid was

purified using a Miniprep kit (Qiagen). After sequencing to verify the correct insertion, the plasmids were linearized using the restriction enzymes, *SpeI* or *Not1*. Single-stranded RNA (ssRNA) was generated using T3 and T7 MEGAscript kits (Thermo Fisher). Equal amounts of the ssRNA were combined to generate a 2 μg/μL solution. The ssRNA was then annealed to form double-stranded (dsRNA) as described by Hughes and Kaufman (2000). The dsRNA and the ssRNAs were run on a gel to verify proper annealing.

dsRNA injections

Fourth instar nymphs were injected with 1 μg (0.5 μL) of *Pc, E(z), jing* and *amp*^{r} dsRNA using a syringe and a pulled borosilicate needle. The dsRNA-treated *O. fasciatus* were then reared at 20°C, 26.5°C or 33°C. Whole bodies of adult *O. fasciatus* were kept frozen at -20°C. The ventral abdomen of each bug was fixed in 3.7% formaldehyde and mounted in a 70% glycerol:30% PBS solution or an 80% glycerol:20% water solution and then imaged.

Analysis of body size and melanization

To examine the effects of knockdowns, dsRNA-injected animals were reared at 26.5°C, and the legs and wings of adults were imaged. For melanization plasticity studies, the total area and melanic pigmented areas of abdominal segments A3 to A5 were measured at each temperature. The proportion of melanization was standardized by dividing the area of melanization by the area of the abdominal segment. The entire area of the forewing and the areas with melanic pigmentation were also measured for each temperature. The area of melanization was normalized by dividing the area of melanic pigmentation by the area of the entire wing. The amount of the orange area on the head was estimated by measuring the linear distance between

the ocelli and the portion of this line that is orange. The amount of melanization in the scutellum was analyzed by measuring the triangular area visible externally and the amount of melanization. All measurements were analyzed using ImageJ (https://imagej.nih.gov/nih-image/). Raw data are available on Dryad (Tan et al., 2024).

Knockdown verification

To verify knockdown of *Pc, E(z)* and *jing, amp^r, Pc, E(z)* and *jing* dsRNA was injected into two fourth instar nymphs each and collected as fifth instar nymphs three days after the molt. cDNA of *amp^r*, *Pc*, *E(z)* and *jing* knockdown animals was synthesized from RNA as described above. Semi-quantitative PCR was performed with *ribosomal protein subunit3* (*RPS3*) serving as a loading control. For *Pc, E(z),* and *jing*, the PCR was run for 30, 35, or 40 cycles. For the *RPS3* primers, the PCR was run for 20, 25 or 30 cycles. Semi-quantitative PCR verified the knockdown of *Pc, E(z)* and *jing* (Fig. S1).

RESULTS

Effects of PcG knockdown on adult morphology

Fourth instar nymphs were injected with *Pc, E(z)* and *jing* dsRNA to determine the effects of PcG gene knockdown on adult phenotypes. At 26.5°C, the *Pc* knockdown adults had increased melanization in the head, the pronotum, the thorax, the wings and the abdomen compared to the *amp^r* dsRNA-injected adults. The heads of the *Pc* knockdowns were missing the orange V-shape pattern that was present in the *amp^r* dsRNA-injected adults (Figs. 1 and 2A). The forewings of *O. fasciatus* develop as hemelytra with a sclerotized proximal section, which is orange with a black band, and a membranous distal section, which is black. In the *Pc* knockdown

nymphs, the melanization of the proximal band was expanded primarily along the veins in the forewing, and only a small portion remained orange (Figs. 1 and 3A). In addition, the forewings of *Pc* knockdown adults had a significantly reduced wing length-to-width ratio compared to the *amp*^{r} dsRNA-injected adults, indicating that the wings were broader than those of the *amp*^{r} dsRNA-injected adults (Fig. S2E); the total wing area was not significantly different from that of *amp*^{r} dsRNA-injected adults (Fig. S2A). The thorax was mostly black with greater expansion of the melanized areas relative to the *amp*^{r} dsRNA-injected controls (Figs. 1A, 4A and 4B). In addition, the morphology of the scutellum was altered such that the scutellum had duller posterior tip compared to the *amp*^{r} dsRNA-injected adults (Fig. 4). In both female and male *Pc* knockdowns, the second abdominal segment had black pigmentation, whereas the *amp*^{r} dsRNA-injected control lacked melanic pigmentation in this segment (Figs. S3 and S4). The fifth abdominal segment in the *Pc* knockdown adults also had larger areas of pigmentation than the *amp*^{r} dsRNA-injected controls. The black bristles on the lateral sides of the abdomen were expanded posteriorly in most of the segments (Figs. S3 and S4, inset). In contrast, in the *amp*^{r} dsRNA-injected control animals, only the anterior portion of each segment had the black bristles on the lateral side of the abdomen (Figs. S3 and S4, inset).

Both the *E(z)* and *jing* knockdown adults had a scutellum with a more pointed tip relative to that of *amp*^{r} dsRNA-injected adults (Fig. 4). In the *E(z)* knockdown adults reared at 26.5°C, the melanization of the head, the thorax and the abdomen was similar to that observed in the *amp*^{r} dsRNA-injected controls (Figs. 1A, 2A, 4A, 4B, S3 and S4). On the wing, however, the proximal melanic band was expanded along the veins although the degree of expansion was much weaker than that of the *Pc* dsRNA-injected animals (Fig. 3A). The *jing* knockdown adults also had limited effects on the adult melanization at 26.5°C. The melanization of the head, the

thorax and the abdomen was similar to that observed in the *amp*^{r} dsRNA-injected controls (Figs. 1A, 2A, 4A, 4B, S3 and S4). On the forewing, the posterior portion of the proximal melanic band was expanded distally such that the black coloration merged with the black membranous portion of the wing (Fig. 3A, arrowhead). Taken together, at 26.5°C, *Pc* knockdown caused a major increase in the melanization of the entire body, while *E(z)* and *jing* knockdown caused a minor expansion of melanization on the wings.

We also examined the morphology of the legs as knockdowns of *Pc* and *E(z)* in a holometabolous insect have been shown to cause partial homeotic transformations of thoracic segment-specific leg identities and tarsus-to-tibia transformations (Chou et al., 2019). We measured the lengths of each leg segment and determined the third thoracic (T3) leg segment-to-first thoracic (T1) leg segment ratios and the T3-to-second thoracic (T2) leg segment ratios (Fig. S5). These ratios did not differ significantly between the knockdown and *amp*^{r} dsRNA-injected adults (Fig. S5C), indicating that at least when injected into fourth instar nymphs, the PcG dsRNAs do not cause homeotic transformations of leg identities. In addition, the tibia-tarsus ratios did not differ between the knockdown adults and the *amp*^{r} dsRNA-injected adults, indicating that the tarsus did not acquire a tibia-like morphology (Fig. S5C). These results demonstrate that the knockdowns of PcG genes had minimal impacts on the leg morphology. The legs can therefore be used as a proxy for body size. Although *E(z)* and *Pc* knockdown adults had slightly increased leg segment lengths, the alterations were minor and inconsistent across different segments (Fig. S5B). Thus, no major changes in body size were noted across the different knockdown animals.

jing *knockdown increases phenotypic plasticity of head melanization*

We next explored the roles of *Pc, E(z)* and *jing* in regulating the temperature-dependent plasticity and robustness of melanic pigmentation. In the *amp*^{r} dsRNA-injected adults, the melanization of the dorsal side decreased at higher temperatures (Figs. 1-4). The heads of the *Pc* knockdown adults were black at all temperatures (Figs. 1 and 2). On the dorsal side, the heads of the *E(z)* and *jing* knockdown adults did not have the orange V-shape pattern and were mostly black at 20°C (Fig. 2A). At higher temperatures, the orange area expanded to be similar to that seen in *amp*^{r} dsRNA-injected animals. To see if the degree of plasticity was increased, the 20°C and 33°C measurements were normalized to the amount of melanization observed at 26.5°C. A two-way ANOVA revealed that there was a statistically significant interaction between the effects of the dsRNA injection and temperature ($F(6, 164) = 4.4121$, $p = 0.0004$) (Table 1). Since *Pc* knockdown heads were completely black at all temperatures, we focused on the reaction norms for *amp*^{r}, *E(z)* and *jing* dsRNA-injected adults (Fig. 2C and D). A comparison of head melanization across the dsRNA treatments showed that the melanization of the head of the *jing* knockdown had the greatest increase in melanization at 20°C relative to the those reared at 26.5°C. The increase in the melanization of *E(z)* knockdown head was statistically indistinguishable from that of the *amp*^{r} dsRNA-injected control heads and the *jing* knockdown heads. At 33°C, no significant differences were observed in the amount of reduction of melanization across the *amp*^{r}, *jing* and *E(z)* dsRNA-injected animals (Fig. 2D). These results demonstrate that *jing* RNAi caused the heads to have increased plasticity. In contrast, because the head of *Pc* knockdown adults were all black at all temperatures, the plasticity was completely removed.

jing *and* E(z) *knockdown increases phenotypic plasticity of wing melanization*

We next examined the effects of these gene knockdowns on the melanization of the forewings. The forewings of normal adults have a black proximal band and a black distal membranous portion. The amount of melanization in the proximal band varied depending on the gene that was knocked down and the temperature. When normalized to the melanization at 26.5°C, there was a statistically significant interaction between the effects of the dsRNA injection and temperature ($F(6, 187) = 7.4752$, $p<0.0001$) (Table 1). *Pc* knockdown led to increased melanization of the wings across all three temperatures and limited plasticity (Fig. 3A). In contrast, plasticity was observed in *amp^r*, *E(z)* and *jing* dsRNA-injected animals. We therefore focused on the amount of melanization in the entire wing for *amp^r*, *E(z)* and *jing* dsRNA-injected animals and found that at 20°C, increased melanization was observed in the *E(z)* and *jing* knockdown adults (Fig. 3A, C, D). At 26.5°C, the wings from *E(z)* knockdown adults had reduced melanization and *jing* knockdown adults had even greater reduction in melanization (Fig. 3A, C, D). At 33°C, *jing* knockdown wings had the least melanization (Fig. 3A, C, D). When normalized to the 26.5°C melanization, the *E(z)* and *jing* knockdown wings had the greatest increase in melanization at 20°C relative to the wings at 26.5°C (Fig. 3D). Overall, forewings from the *jing* knockdown adults exhibited the greatest amount of plasticity although *E(*z) knockdown adults also exhibited higher plasticity than *amp^r* dsRNA-injected adults. Although the *Pc* knockdown animals exhibited altered melanization in the hindwings, the hindwings – which are normally hidden behind the forewings – overall did not exhibit obvious changes in melanization across temperatures for any of the knockdown treatments (Fig. S6).

jing *RNAi increases phenotypic plasticity of thoracic melanization*

Jing knockdown adults exhibited thoracic melanization plasticity whereas *E(z)* and *Pc* knockdown did not appear to increase in plasticity (Fig. 4). *Pc* knockdown adults had increased melanization in their thoraces across all temperatures and were mostly black (Fig. 4). Because only *jing* knockdown adults showed notable changes in plasticity relative to the *amp*^{r} dsRNA-injected adults, we focused on *jing* knockdown adults. To quantify the plasticity in the *jing* knockdown thorax, the scutellum was isolated and the amount of melanization was quantified. Compared to the *amp*^{r} dsRNA-injected adults, the *jing* knockdown adult had decreased melanization at 33°C (Fig. 4A, B, D, E). When normalized to the melanization at 26.5°C, *jing* exhibited significantly higher amount of melanization at 20°C and significantly reduced melanization at 33°C (Fig. 4E). The interaction between the effects of the dsRNA injection and temperature was statistically significant ($F(2, 70) = 18.4331$, $p<0.0001$) (Table 1). Thus, the removal of *jing* led to an increased plasticity in the scutellum. The ventral thorax of *jing* knockdown adults was also observed to be mostly devoid of melanization at 33°C, indicating that *jing* normally maintains robustness of melanization in the thorax.

Segment specific effects of jing*,* E(z) *and* Pc *RNAi on ventral abdominal pigmentation plasticity*

The abdomens of *O. fasciatus* are sexually dimorphic. Therefore, the males and females were analyzed separately. In the *amp*^{r} dsRNA-injected females, at 26.5°C, the females typically have one large band in A3 and 2 spots in A4 (Fig. S3). At 20°C, these melanic patterns expanded and two additional spots appeared in both A2 and A5. At 33°C, two spots developed in A3 and A4 (Fig. S3). In the males, at 26.5°C, bands developed in A3 and A4 (Fig. S4). At 20°C, the bands expanded, and two additional spots appeared in A2 and A5 (Fig. S4). At 33°C, two spots developed in A3 and A4 (Fig. S4). In addition, on the lateral sides of each of the abdominal

segment, small black spots developed on the anterior portion along the lateral margins of each segment (insets in Figs. S3 and S4).

In both the male and female abdominal segments of *Pc* knockdowns, abdominal segments 2 through 5 (A2-A5) developed large bands at 20°C unlike other knockdown animals (Figs. S3 and S4). At both 26.5 and 33°C, two melanic spots appeared on A2 through A4 of the female. In the males reared at 26.5°C, two bands developed on A3 and A4 (Fig. S4). At 33°C, two spots developed on A3 and A4 (Fig. S4), and occasionally also on A2 (not shown). For both females and males, the melanic marks on the anterior portion of the lateral margins were expanded posteriorly (insets in Figs. S3 and S4).

In the *E(z)* knockdown adults, the plasticity in abdominal melanization was similar to that of amp^r dsRNA-injected adults (Figs. S3, S4, S7B and S8). Measurements of melanized area normalized to the measurements at 26.5°C demonstrated that the change in melanization was similar to that seen in amp^r dsRNA-injected adults except in the A5 where females exhibited greater plasticity and males exhibited less plasticity compared to the amp^r dsRNA-injected adults (Fig. S8). In the *jing* knockdown adults, increased plasticity was seen in A3 for both sexes and in A4 for the males (Fig. S8). Overall, no consistent change in plasticity was observed in the ventral abdominal melanization.

DISCUSSION

Canalization is an important mechanism by which organisms evolve developmental stability and robustness. For traits like aposematic coloration, evolution of robust phenotypic development amid environmental fluctuations may contribute to increased survival and fitness. In this study, we explored the potential role of epigenetic regulation on adult melanin plasticity and robustness in *O. fasciatus*.

Pc is involved with patterning in the abdomen and wings

The knockdown of *Pc* led to significantly more melanization in the second and fifth abdominal segments, the lateral edge of each abdominal segment, the head and the forewings. The pigmentation of *O. fasciatus* in the body overall is regulated by the melanin pathway, in which dopamine is converted to the black melanin (Liu et al., 2014). Our head and the abdomen of the *Pc* knockdown nymphs resemble those seen when *ebony* and *black* are knocked down (Liu et al., 2016). Ebony and black both play a role in N-β-alanyldopamine (NBAD) synthesis, and knockdown of *ebony* or *black* leads to an increased amount of dopamine and melanization (Liu et al., 2016). Thus, *Pc* may be involved in reducing melanin synthesis and may promote the production of NBAD instead. In the *ebony* and *black* knockdowns, the orange areas of the wings were darker such that the entire wing became black. In contrast, when *Pc* was knocked down, the shape of the melanic pattern was altered. This indicates that Pc may be involved in regulating the establishment of the pattern in addition to reducing melanin synthesis. Alternatively, because the veins supply melanin (Liu et al., 2014) and *Pc* knockdown leads to an expansion of the melanization along the veins, *Pc* may impact how much melanin precursor is transported through the veins.

E(z) and Jing buffer against temperature fluctuation

Although Pc repressed overall melanization across all temperatures, it did not appear to regulate phenotypic plasticity as knockdown of *Pc* led to consistently increased melanization across all temperatures. In contrast, the dorsal melanization of *E(z)* and *jing* knockdown adults exhibited increased sensitivity to temperature. *E(z)* and *jing* knockdowns exhibited increased temperature-dependent phenotypic plasticity in the wings compared to the *Pc* knockdown and the control animals (Fig. 3). *jing* knockdown, in particular, increased the amount of plasticity

exhibited in various tissues, including the head (Fig. 2) and the thorax (Fig. 4). *jing* has also previously been shown to be involved in regulating abdominal pigmentation of *D. melanogaster* (Culi et al., 2006). These observations suggest that *E(z)* and *jing* play a role in maintaining robustness of melanization. Previous research has also shown that epigenetic regulators like histone deacetylases (HDACs) and PcG proteins play a role in the nutrition-sensitive plasticity of the mandibles of male beetles *Gnatocerus cornutus* (Ozawa et al., 2016). Thus, PcGs may play important roles in the process of canalization and the evolution of plasticity.

PcG regulated genes have been shown to evolve through temperature-dependent selection. Studies of different *D. melanogaster* populations have demonstrated that the temperature-sensitivity of PcG target genes have diverged between tropical and temperate regions with reduced plasticity found in populations from temperate regions (Voigt and Kost, 2021; Voigt and Froschauer, 2023). In addition, variants of the PcG genes themselves have been shown to be under selection in northern temperate populations of *D. melanogaster*, leading to the evolution of thermal plasticity (Gibert et al., 2011). Thus, PcG genes and their targets can evolve to shape phenotypic plasticity and robustness.

At this point, we do not know which genes are regulated by PcGs in *O. fasciatus*. Because PcGs generally repress gene expression, we propose that PRC2 may repress melanization genes at lower temperatures in the head and the wings. When *E(z)* or *jing* are knocked down, gene expression is de-repressed at lower temperatures, leading to increased melanization of the head and wings. In *D. melanogaster*, abdominal pigment plasticity has been shown to be regulated by *tan*, a gene encoding N-β-alanyldopamine hydrolase, which catalyzes the hydrolysis of NBAD to dopamine (Gibert et al., 2016; True et al., 2005). The promoter of *tan*

is highly acetylated at low temperatures, leading to darker pigmentation (Gibert et al., 2016). Whether or not *tan* is regulated by PcGs in *O. fasciatus* remains to be seen.

Histone modification as a key contributor to tissue-specific canalization of traits

In this study, we demonstrated the importance of E(z) and Jing in maintaining robustness of the dorsal pigmentation. The orange and black pigmentation of *Oncopeltus* serves as warning coloration to deter potential predators. We propose that robustness of the dorsal pigmentation is essential for predators' ability to recognize the aposematic color patterns and that PcG genes and/or their targets may have played an important role in canalizing the phenotypes across various temperatures. In contrast, the ventral abdominal patterns, which likely are not under similar selective pressures by predators, were highly variable and not consistently impacted when components of PRC2 were knocked down. Similarly, the hindwings did not exhibit any detectable changes in melanization. Thus, epigenetic regulators may evolve in a tissue-specific manner to confer robustness and plasticity to specific traits. We propose that the evolution of robustness in aposematic coloration and possibly more broadly in other traits involve evolution of histone modifiers. Therefore, studies on robustness would benefit from consideration of histone modification.

Acknowledgements

We thank the two anonymous reviewers for their constructive comments on the manuscript and the members of the Suzuki lab for their assistance throughout the project.

Funding sources

This work was supported by the National Science Foundation grant IOS-2002354, the Dorothy and Charles Jenkins Distinguished Chair in Science funds to YS, and funds provided by Wellesley College.

References

Bantignies, F., Grimaud, C., Lavrov, S., Gabut, M., Cavalli, G., 2003. Inheritance of Polycomb-dependent chromosomal interactions in Drosophila. Genes Dev. 17, 2406–2420.

Berenbaum, M.R., Miliczky, E., 1984. Mantids and milkweed bugs: efficacy of aposematic coloration against invertebrate predators. Am. Midl. Nat. 64–68.

Cao, R., Wang, L. J., Wang, H. B., Xia, L., Erdjument-Bromage, H., Tempst, P., Jones, R. S., & Zhang, Y. (2002). Role of histone H3 lysine 27 methylation in polycomb-group silencing. *Science*, *298*(5595), 1039–1043. https://doi.org/10.1126/science.1076997

Chan, C.-S., Rastelli, L., Pirrotta, V., 1994. A Polycomb response element in the Ubx gene that determines an epigenetically inherited state of repression. EMBO J. 13, 2553–2564.

Chou, J., Ferris, A.C., Chen, T., Seok, R., Yoon, D., Suzuki, Y., 2019. Roles of Polycomb group proteins Enhancer of zeste (E(z)) and Polycomb (Pc) during metamorphosis and larval leg regeneration in the flour beetle Tribolium castaneum. Dev Biol 450, 34–46. https://doi.org/10.1016/j.ydbio.2019.03.002

Ciabrelli, F., Comoglio, F., Fellous, S., Bonev, B., Ninova, M., Szabo, Q., Xuéreb, A., Klopp, C., Aravin, A., Paro, R., 2017. Stable Polycomb-dependent transgenerational inheritance of chromatin states in Drosophila. Nat. Genet. 49, 876–886.

Culi, J., Aroca, P., Modolell, J., Mann, R.S., 2006. jing is required for wing development and to establish the proximo-distal axis of the leg in Drosophila melanogaster. Genetics 173, 255–266.

Czermin, B., Melfi, R., McCabe, D., Seitz, V., Imhof, A., & Pirrotta, V. (2002). Drosophila enhancer of Zeste/ESC complexes have a histone H3 methyltransferase activity that marks chromosomal Polycomb sites. *Cell*, *111*(2), 185–196.

Fabricant, S.A., Burdfield-Steel, E.R., Umbers, K., Lowe, E.C., Herberstein, M.E., 2018. Warning signal plasticity in hibiscus harlequin bugs. Evol. Ecol. 32, 489–507.

Fauvarque, M.-O., Dura, J.-M., 1993. polyhomeotic regulatory sequences induce developmental regulator-dependent variegation and targeted P-element insertions in Drosophila. Genes Dev. 7, 1508–1520.

Fischer, S., Weber, L.M., Liefke, R., 2022. Evolutionary adaptation of the Polycomb repressive complex 2. Epigenetics Chromatin 15, 7 https://doi.org/10.1186/s13072-022-00439-6

Francis, N.J., Saurin, A.J., Shao, Z., Kingston, R.E., 2001. Reconstitution of a functional core polycomb repressive complex. Mol. Cell 8, 545–56.

Gibert, J.-M., Karch, F., Schlötterer, C., 2011. Segregating variation in the polycomb group gene cramped alters the effect of temperature on multiple traits. PLoS Genet. 7, e1001280.

Gibert, J.-M., Mouchel-Vielh, E., De Castro, S., Peronnet, F., 2016. Phenotypic plasticity through transcriptional regulation of the evolutionary hotspot gene tan in Drosophila melanogaster. PLoS Genet. 12, e1006218.

Gibert, J.-M., Peronnet, F., Schlötterer, C., 2007. Phenotypic plasticity in Drosophila pigmentation caused by temperature sensitivity of a chromatin regulator network. PLoS Genet. 3, e30.

Guilford, T., 1988. The evolution of conspicuous coloration. Am. Nat. 131, S7–S21.

Harr, B., Kauer, M., Schlötterer, C., 2002. Hitchhiking mapping: a population-based fine-mapping strategy for adaptive mutations in Drosophila melanogaster. Proc. Natl. Acad. Sci. 99, 12949–12954.

Harvey, P.H., Bull, J.J., Pemberton, M., Paxton, R.J., 1982. The evolution of aposematic coloration in distasteful prey: a family model. Am. Nat. 119, 710–719.

Hughes, C.L., Kaufman, T.C., 2000. RNAi analysis of Deformed, proboscipedia and Sex combs reduced in the milkweed bug Oncopeltus fasciatus: novel roles for Hox genes in the hemipteran head. Development. 127, 3683–3694.

Kassis, J.A., Kennison, J.A., Tamkun, J.W., 2017. Polycomb and trithorax group genes in Drosophila. Genetics 206, 1699–1725.

Levine, M.T., Begun, D.J., 2008. Evidence of spatially varying selection acting on four chromatin-remodeling loci in Drosophila melanogaster. Genetics 179, 475–485.

Lindstedt, C., Lindström, L., Mappes, J., 2009. Thermoregulation constrains effective warning signal expression. Evolution 63, 469–478.

Lindstedt, C., Talsma, J.H.R., Ihalainen, E., Lindström, L., Mappes, J., 2010. Diet quality affects warning coloration indirectly: excretion costs in a generalist herbivore. Evolution 64, 68–78.

Liu, J., Lemonds, T.R., Marden, J.H., Popadic, A., 2016. A Pathway Analysis of Melanin Patterning in a Hemimetabolous Insect. Genetics 203, 403–13. https://doi.org/10.1534/genetics.115.186684

Liu, J., Lemonds, T.R., Popadic, A., 2014. The genetic control of aposematic black pigmentation in hemimetabolous insects: insights from Oncopeltus fasciatus. Evol Dev 16, 270–7. https://doi.org/10.1111/ede.12090

Loeffler-Henry, K., Kang, C., & Sherratt, T. N. (2023). Evolutionary transitions from camouflage to aposematism: Hidden signals play a pivotal role. *Science*, 379, 1136–1140.

Mallet, J., 1989. The genetics of warning colour in Peruvian hybrid zones of Heliconius erato and H. melpomene. Proc. R. Soc. Lond. B Biol. Sci. 236, 163–185.

Matsuoka, Y., Bando, T., Watanabe, T., Ishimaru, Y., Noji, S., Popadic, A., Mito, T., 2015.

Short germ insects utilize both the ancestral and derived mode of Polycomb group-mediated epigenetic silencing of Hox genes. Biol. Open 4, 702–709. https://doi.org/10.1242/bio.201411064

Muller, J., Hart, C.M., Francis, N.J., Vargas, M.L., Sengupta, A., Wild, B., Miller, E.L., O'Connor, M.B., Kingston, R.E., Simon, J.A., 2002. Histone methyltransferase activity of a Drosophila Polycomb group repressor complex. Cell 111, 197–208.

Nokelainen, O., Lindstedt, C., Mappes, J., 2013. Environment-mediated morph-linked immune and life-history responses in the aposematic wood tiger moth. J. Anim. Ecol. 82, 653–662.

Novak V.I.A., 1955. To the knowledge of the mechanisms conditioning the development of the ventral black pattern in the abdomen of the bug Oncopeltus fasciatus. Vestn. Cesk. Spolecnosti. Zool. 19, 233–246.

Ozawa, T., Mizuhara, T., Arata, M., Shimada, M., Niimi, T., Okada, K., Okada, Y., Ohta, K., 2016. Histone deacetylases control module-specific phenotypic plasticity in beetle weapons. Proc. Natl. Acad. Sci. 113, 15042–15047.

Prudic, K.L., Skemp, A.K., Papaj, D.R., 2007. Aposematic coloration, luminance contrast, and the benefits of conspicuousness. Behav. Ecol. 18, 41–46.

Sedaghat, Y., Miranda, W.F., Sonnenfeld, M.J., 2002. The jing Zn-finger transcription factor is a mediator of cellular differentiation in the Drosophila CNS midline and trachea.

Shao, Z., Raible, F., Mollaaghababa, R., Guyon, J.R., Wu, C.T., Bender, W., Kingston, R.E., 1999. Stabilization of chromatin structure by PRC1, a Polycomb complex. Cell 98, 37–46. https://doi.org/10.1016/S0092-8674(00)80604-2

Sharma, A.I., Yanes, K.O., Jin, L., Garvey, S.L., Taha, S.M., Suzuki, Y., 2016. The phenotypic

plasticity of developmental modules. Evodevo 7, 15. https://doi.org/10.1186/s13227-016-0053-7

Sillen-Tullberg, B., Bryant, E.H., 1983. The evolution of aposematic coloration in distasteful prey: an individual selection model. Evolution 993–1000.

Stevens, M., Ruxton, G.D., 2012. Linking the evolution and form of warning coloration in nature. Proc. R. Soc. B Biol. Sci. 279, 417–426.

Sword, G.A., 2002. A role for phenotypic plasticity in the evolution of aposematism. Proc. R. Soc. Lond. B Biol. Sci. 269, 1639–1644.

Tan, M et al. 2024. Data from: Effects of PcG gene knockdowns on adult morphology [Dataset]. Dryad. https://doi.org/10.5061/dryad.f7m0cfz51

True, J.R., Yeh, S.-D., Hovemann, B.T., Kemme, T., Meinertzhagen, I.A., Edwards, T.N., Liou, S.-R., Han, Q., Li, J., 2005. Drosophila tan encodes a novel hydrolase required in pigmentation and vision. PLoS Genet. 1, e63.

Turner, B. M. 2009. Epigenetic responses to environmental change and their evolutionary implications. *Philos. Trans. R. Soc. B: Biol. 364*, 3403–3418.

Vogt, G., 2022. Epigenetics and phenotypic plasticity in animals, in: Epigenetics, Development, Ecology and Evolution. Springer, pp. 35–108.

Voigt, S., Froschauer, C., 2023. Genome-wide temperature-sensitivity of Polycomb group regulation and reduction thereof in temperate Drosophila melanogaster. Genetics 224, iyad075.

Voigt, S., Laurent, S., Litovchenko, M., Stephan, W., 2015. Positive selection at the polyhomeotic locus led to decreased thermosensitivity of gene expression in temperate Drosophila melanogaster. Genetics 200, 591–599.

Waddington, C. H. 1942. Canalization of development and the inheritance of acquired characters. Nature 150, 563–565.

Waddington, C. H. 1953. Genetic assimilation of an acquired character. Evolution 7, 118–126.

Waddington, C. H. 1956. Genetic assimilation of the bithorax phenotype. Evolution 10, 1–13.

Wang, H., Wang, L., Erdjument-Bromage, H., Vidal, M., Tempst P., Jones, R. S., Zhang, Y., 2004. Role of histone H2A ubiquitination in Polycomb silencing. Nature 431, 873–878.

519 **TABLE**

520 Table 1. Two-way ANOVA results.

		DF	F	P-value
Head	Gene	3	0.6214	0.6021
	Temperature	2	67.695	<.0001
	Gene X Temperature	6	4.4121	0.0004
Wing	Gene	3	7.7871	<.0001
	Temperature	2	65.4683	<.0001
	Gene X Temperature	6	7.4752	<.0001
Scutellum	Gene	1	4.4451	0.0386
	Temperature	2	33.2042	<.0001
	Gene X Temperature	2	18.4331	<.0001
A3 female	Gene	3	6.2111	0.0007
	Temperature	2	142.7434	<.0001
	Gene X Temperature	6	9.3711	<.0001
A4 female	Gene	3	2.0669	0.1098
	Temperature	2	73.01	<.0001
	Gene X Temperature	6	1.7372	0.1207
A5 female	Gene	3	6.3473	0.0006
	Temperature	2	16.4447	<.0001
	Gene X Temperature	6	7.2443	<.0001
A3 male	Gene	3	1.5204	0.2159
	Temperature	2	117.3304	<.0001
	Gene X Temperature	6	6.087	<.0001
A4 male	Gene	3	0.9735	0.4097
	Temperature	2	95.0001	<.0001
	Gene X Temperature	6	4.9816	0.0002
A5 male	Gene	3	4.8241	0.0039
	Temperature	2	25.5526	<.0001
	Gene X Temperature	6	5.2587	0.0001

521

522

FIGURE LEGENDS

Figure 1. Effect of *Pc, E(z)* and *jing* knockdown on adult phenotypes at 20°C, 26.5°C and 33°C. Dorsal (left) and ventral (right) whole body views of the *Pc* knockdown, *E(z)* knockdown, *jing* knockdown and *amp^r* dsRNA-injected control of female *O. fasciatus* at various temperatures.

Figure 2. Pigmentation plasticity of the head. (A) The heads of *amp^r*, *Pc*, *E(z)* and *jing* dsRNA-injected adults reared at different temperatures. (B) Measurement of head melanization. (C) Reaction norms of head melanization. (D) Normalized amounts of head melanization. The amount of head melanization for each treatment was divided by the average amount of melanization for the respective knockdowns at 26.5°C. Results of the one-way ANOVA with Tukey HSD conducted for values at 20°C and 33°C are represented by the letters where distinct letters indicate statistically significant differences.

Figure 3. The *E(z)* and *jing* knockdowns had increased plasticity of melanization in the forewings compared to the *amp^r* dsRNA-injected adults. (A) Forewings of *amp^r, Pc*, *E(z)* and *jing* dsRNA-injected *O. fasciatus* at different temperatures. The arrowhead indicates the melanin in the proximal band blending with the melanized membranous portion of the forewing. (B) Diagram showing the area measured to determine the amount of melanization of the wings. The proportion was calculated by measuring the total melanized area and dividing it by the total area of the forewing. (C) *E(z)* and *jing* knockdown wings had increased plasticity in the forewings as a function of temperature. (D) Normalized amount of forewing melanization. The amount of

546 melanization for each treatment was divided by the average amount of melanization for the
547 respective knockdowns at 26.5°C. Results of the one-way ANOVA with Tukey HSD conducted
548 for values at 20°C and 33°C are represented by the letters where distinct letters indicate
549 statistically significant differences.
550
551 **Figure 4. The effects of *amp^r*, *Pc*, *E(z)* and *jing* dsRNA injections on the thoracic segments.**
552 (A, B) The dorsal (A) and ventral (B) views of the animals at different temperatures. (C) The
553 measurements taken to determine the amount of melanization on the scutellum. (D) Quantified
554 amount of melanization for *amp^r* and *jing* dsRNA-injected adults. (E) Amount of melanization
555 normalized to the amount of melanization at 26.5°C. Asterisks indicate statistically significant
556 differences (Student t-test, $p<0.0001$).
557
558

Figure 1

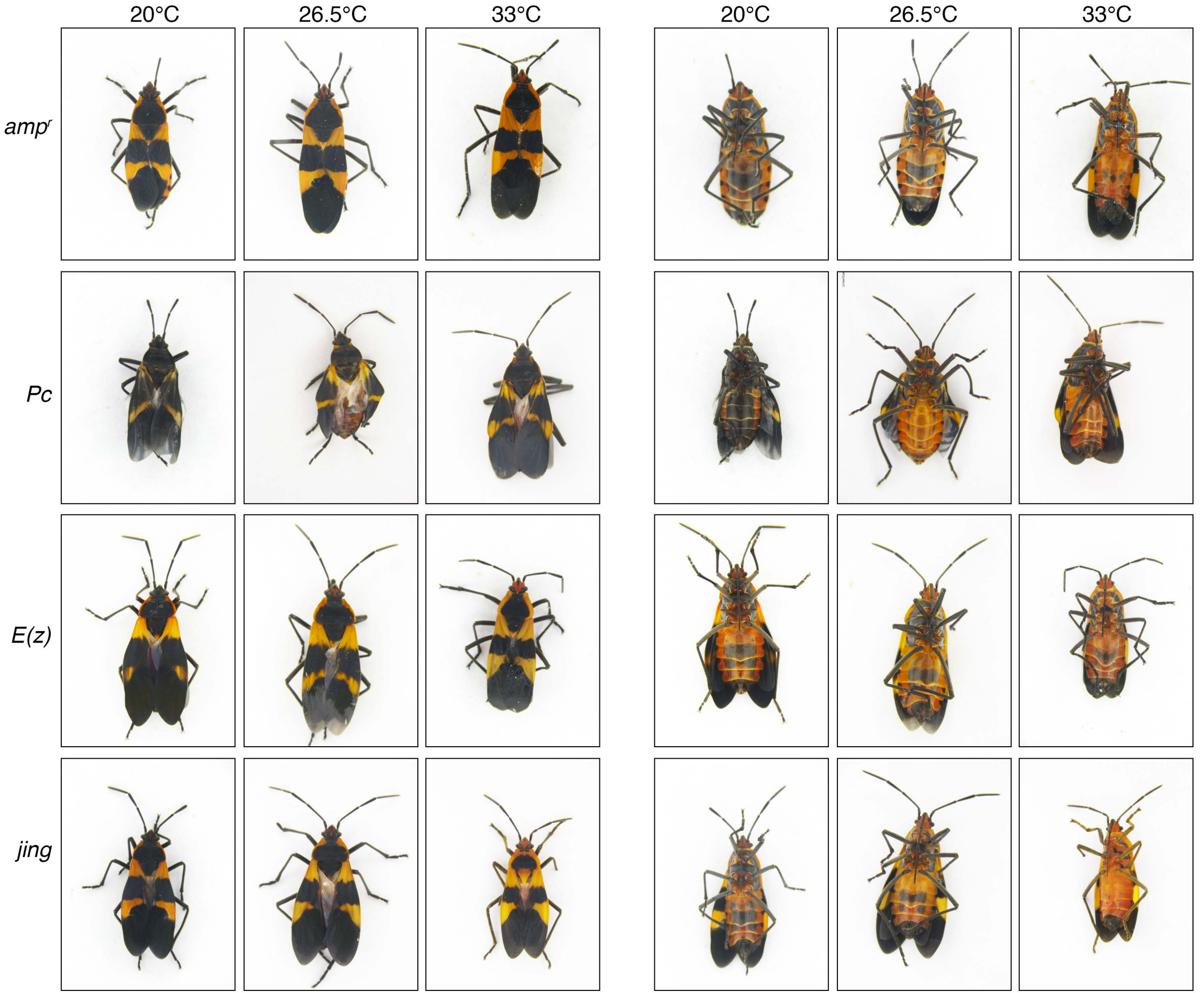

Figure 2

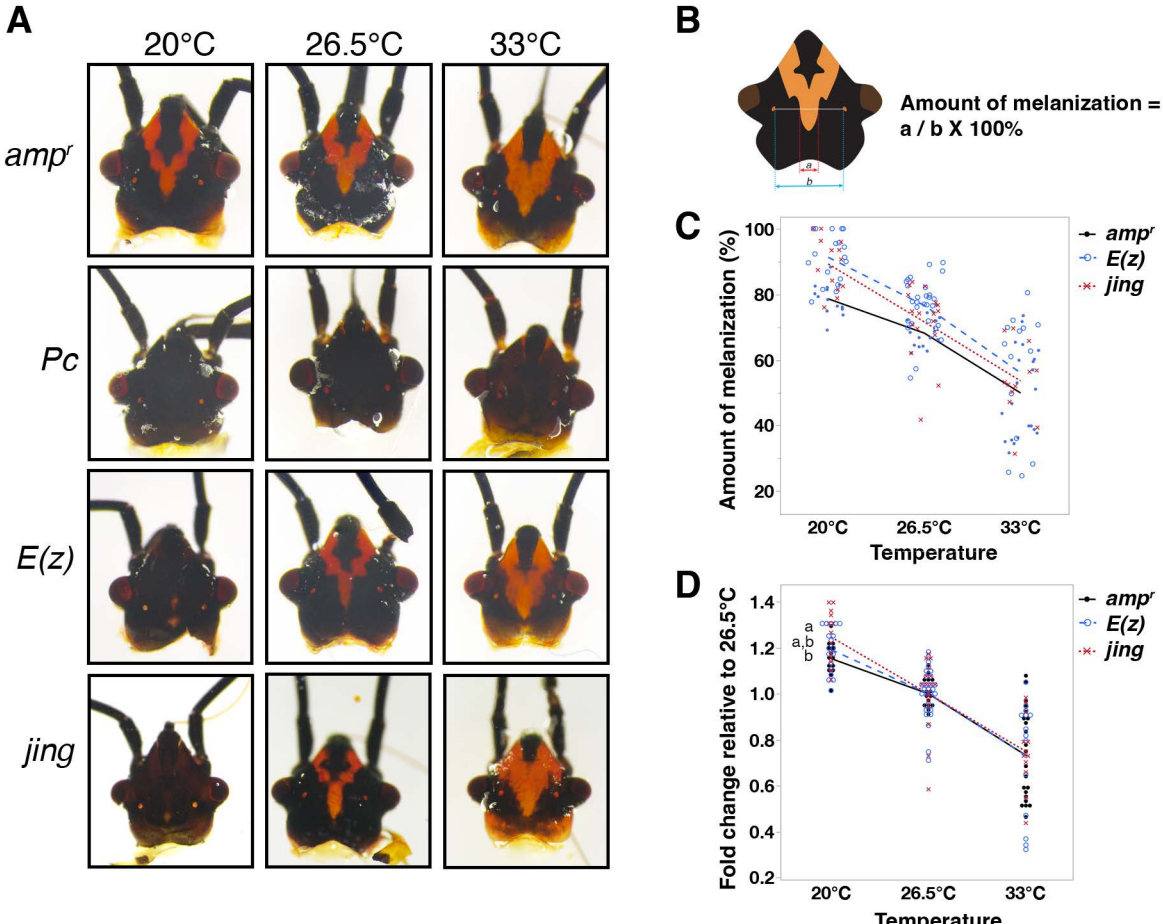
A
20°C
26.5°C
33°C
amp^r
Pc
E(z)
jing
B
Amount of melanization =
a / b X 100%
a
b
C
Amount of melanization (%)
100
80
60
40
20
20°C
26.5°C
33°C
Temperature
amp^r
E(z)
jing
D
Fold change relative to 26.5°C
1.4
1.2
1.0
0.8
0.6
0.4
0.2
a
a,b
b
20°C
26.5°C
33°C
Temperature
amp^r
E(z)
jing

Figure 3

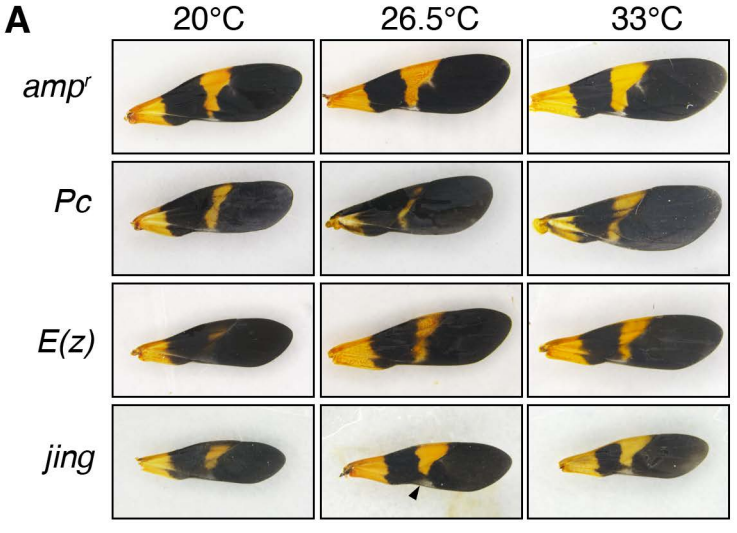

Amount of melanization =
Σ(a) / total wing area X 100%

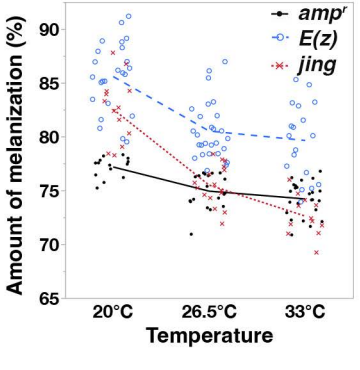

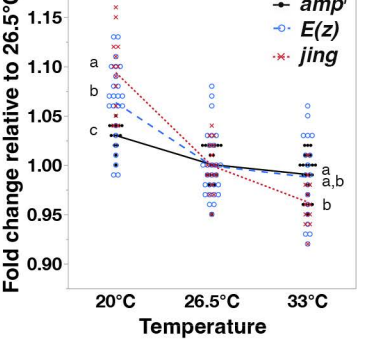

Figure 4

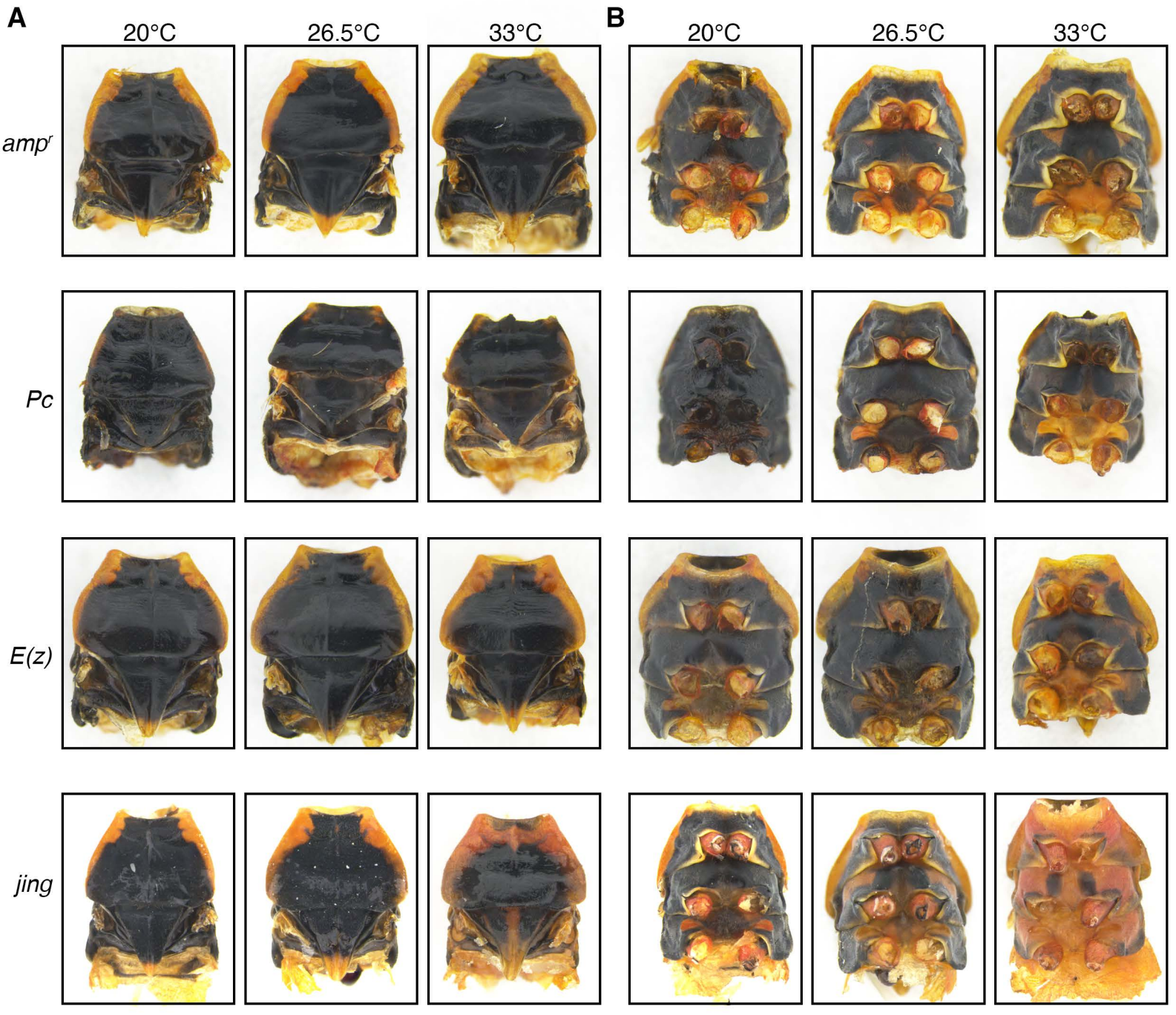

C

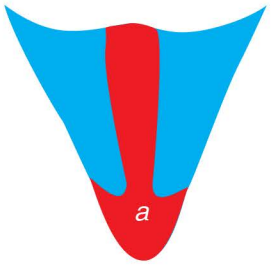

Amount of melanization =
a / total scutellum area X 100%

D

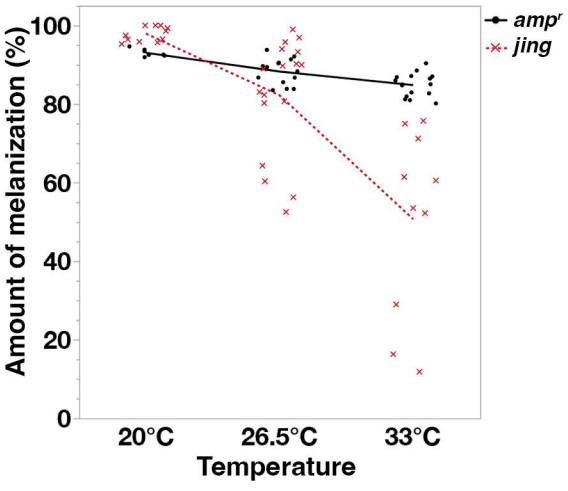

E